Propagation and mode conversion of lower-hybrid waves generated by a finite source

P. M. Bellan and M. Porkolab

Plasma Physics Laboratory, Princeton University, Princeton, New Jersey 08540

(Received 4 February 1974)

The propagation of electrostatic plasma waves, and their subsequent conversion into hot plasma waves at the lower hybrid frequency is calculated for realistic density profiles and finite rf sources in a slab geometry. A finite length slow wave source having a potential distribution $\phi \sim \cos k_0 z$ is found to generate spatial oscillations having a well-defined wavelength. These oscillations are confined to regions bounded by conical curves originating at the ends of the source. The axial distance of rf energy propagation to the lower hybrid layer is found to be greater than the radial distance of propagation by a factor of the order $(m_i/m_e)^{1/2}$. The conversion at the lower hybrid layer of the electrostatic cold plasma waves excited by a finite source into propagating hot plasma waves is calculated. It is shown that collisional damping at the lower hybrid layer may predominate over mode conversion even for relatively low collision frequencies.

I. INTRODUCTION

Cold plasma waves excited by an rf source external to a magnetically confined plasma propagate into the plasma with continuously decreasing wavelengths until they reach the lower hybrid resonant layer. This resonant layer exists in the region where the ion plasma frequency is typically the order of the wave frequency. Stix showed that just before the hybrid layer the incoming cold plasma wave may convert into a short wavelength hot plasma wave.[1] Beyond the hybrid layer both hot and cold plasma waves are evanescent. The hot plasma waves propagate back toward the plasma boundary and are highly damped by collisional and/or collisionless processes. These effects are of great practical interest since they offer the possibility of heating plasmas in fusion reactors with readily available gigahertz high power rf sources. The usual infinite homogeneous plasma theory is not adequate to describe these waves.[2] In particular, since the dispersion relation depends strongly on density, inhomogeneities of density are expected to play an important role in wave propagation. In addition, the boundary conditions imposed by a necessarily finite rf source are expected to have a strong effect on the incoming cold plasma wave, and hence on the converted hot plasma wave.

Kuehl has shown theoretically that the electrostatic plasma wave field generated by a point source consists of a double cone singularity with axis along the magnetic field.[3] Fisher and Gould[4] have experimentally verified this picture for electron plasma waves in a homogeneous plasma. Briggs and Parker[5] have shown theoretically and experimentally that in an inhomogeneous plasma lower hybrid waves excited by a point source have a conical trajectory which bends relative to the magnetic field so that at the resonant layer it is parallel to the magnetic field. The WKB approximation which they used provides solutions for plasmas of moderate density gradients, but these solutions become invalid near the lower hybrid layer and near the plasma boundary.

The purpose of this paper is (i) to determine the domain of validity of the WKB solution of Ref. 5 and establish the behavior of the exact solution when the WKB solution is invalid and (ii) to show, for cases when the WKB method is valid, the exact structure of both the incoming cold and the outgoing converted hot plasma waves excited by a source of finite physical dimensions. In particular, we will examine certain aspects of lower hybrid wave propagations which are of importance in interpreting realistic experimental situations.[6,7]

The plan of the paper is as follows: In Sec. II we derive a criterion for WKB validity that involves the density e-folding scale length, and we obtain a solution for plasmas having density gradients steep enough to violate this criterion. In Sec. III we show the effects of finite rf sources upon cold plasma wave propagation. In Sec. IV we review the process of conversion of the incoming cold plasma wave to a hot plasma wave near the lower hybrid layer, and in Sec. V these calculated results are extended to include collisional effects. In Sec. VI the results of Secs. III–V are used to obtain the hot plasma waves resulting from the conversion of cold plasma waves driven by a finite rf source. In Sec. VII a summary is given.

II. COLD PLASMA WAVE EQUATION

We shall consider a plasma with a uniform magnetic field in the z direction and a density gradient in the x direction. An rf generator emitting waves with time dependence $\exp(-i\omega t)$ is located just outside the plasma. The frequency ω is chosen such that $\omega_{ci} \ll \omega \ll \omega_{ce}$, where ω_{ci} and ω_{ce} are the ion and electron cyclotron frequencies, respectively. The cold plasma dielectric tensor is a function of x and its nonzero elements are given approximately by the following expressions:

$$K_{xx} = 1 - \omega_{pi}^2/\omega^2 + \omega_{pe}^2/\omega_{ce}^2,$$
$$K_{xy} = -K_{yx} = -i\omega_{pe}^2/\omega\omega_{ce},$$
$$K_{zz} = 1 - \omega_{pe}^2/\omega^2, \qquad (1)$$

where ω_{pi} and ω_{pe} are the ion and electron plasma frequencies, respectively. We define $x = 0$ by $K_{xx}(0) = 0$; thus, $x = 0$ is the position of the lower hybrid layer. In this coordinate system the rf source is located at $x = x_s$, as shown in Fig. 1.

If a z dependence of $\exp(ik_z z)$ is also assumed for the

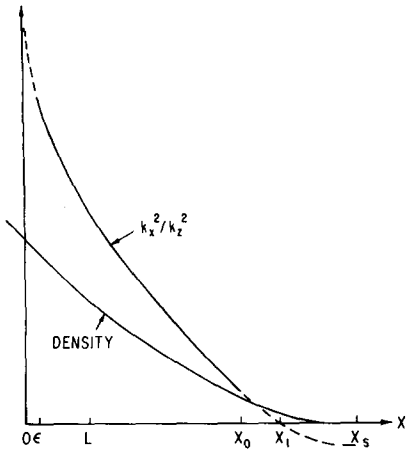

FIG. 1. Density and k_z^2 vs x; $K_{xx} = 0$ at $x = 0$; the symbols are defined in the text. The solid line for k_z^2 shows where the WKB approximation may be used.

generator, and $ck_z/\omega \gg 1$, the differential equations describing slow waves in the plasma are given by[5]

$$\frac{d}{dx}\left(K_{xx}\frac{dE_z}{dx}\right) - k_z^2 K_{zz} E_z = 0 \tag{2}$$

and

$$E_x = \frac{1}{ik_z}\frac{dE_z}{dx}. \tag{3}$$

Since Eqs. (2) and (3) involve E_x and E_z, we observe that this mode couples to the transverse magnetic mode at the plasma vacuum boundary.[8,9] We note that a transverse electric mode converts into a fast wave which does not have a resonance at the lower hybrid layer.[8]

A. Homogeneous plasma theory

Equation (2) predicts the dispersion relation

$$k_x^2/k_z^2 = -K_{zz}/K_{xx} \tag{4}$$

for electrostatic cold plasma waves in an infinite homogeneous plasma. The magnitude of $\mathbf{k}$ does not appear in Eq. (4); instead Eq. (4) determines the direction of $\mathbf{k}$. This means that in order for a wave to have a well-defined k_x it *must* have a well-defined k_z. Equation (4) also states that k_x^2/k_z^2 is infinite if the plasma density and ω are such that $K_{xx} = 0$. Although the Fourier analysis used to obtain Eq. (4) is only valid for a homogeneous plasma, we may expect similar behavior of k_x in a moderately inhomogeneous plasma.

B. Inhomogeneous plasma theory

Using Eq. (4) to give the local value of k_x, Eq. (2) may be solved using the WKB method:[5]

$$E_z(x, k_z) = E_z(x_0, k_z) A(x, x_0) \exp[i \mid k_z \mid g(x)], \tag{5}$$

where

$$g(x) = \int_{x_0}^{x}\left(-\frac{K_{zz}(x')}{K_{xx}(x')}\right)^{1/2} dx' \tag{6}$$

and

$$A(x, x_0) = \left(\frac{K_{xx}(x_0)K_{zz}(x_0)}{K_{xx}(x)K_{zz}(x)}\right)^{1/4}. \tag{7}$$

The WKB method is valid only when

$$k_x^{-1}\frac{dk_x}{dx} \ll k_x. \tag{8}$$

The starting point, x_0, must lie in a region where Eq. (8) is satisfied.

Let us examine the requirements for Eq. (8) to be satisfied, and hence the WKB solution to be valid. In order to calculate dk_x/dx, we must choose a particular density profile. We choose an exponential profile since (i) it is similar to experimental density profiles, (ii) it is convenient to work with analytically, and (iii) when Eq. (8) is violated, it is possible to find exact solutions of Eq. (2). We thus assume a density profile $n = n_{LH}\exp(-x/L)$, where n_{LH} is the density at $x = 0$ and L is the density e-folding scale length.

By defining the dimensionless variables

$$\beta = \frac{m_e}{m_i}\left(1 - \frac{\omega^2}{\mid \omega_{ci}\omega_{ce} \mid}\right) \tag{9}$$

and

$$w = \exp[-x/L] \tag{10}$$

Eq. (4) becomes

$$\frac{k_x^2}{k_z^2} = -\frac{(1 - w/\beta)}{1 - w}. \tag{11}$$

Using Eq. (10) and (11) to calculate dk_x/dx, we find that Eq. (8) is equivalent to

$$w^2\frac{\beta}{(2k_zL)^2} \ll (1 - w)(w - \beta)^3. \tag{12}$$

Equation (12), and thus Eq. (8), may be satisfied only if

$$k_zL \gg \beta^{1/2} \tag{13}$$

and, if this is so, only when

$$\frac{\beta}{(2k_zL)^2} \ll w \ll 1 - \frac{\beta}{(2k_zL)^2}. \tag{14}$$

Using Eq. (10) and defining x_1 by $K_{zz}(x_1) = 0$, we find Eq. (14) is equivalent to

$$\frac{\beta}{(2k_zL)^2} \ll x \ll x_1 - 2L\ln\frac{1}{(2k_zL)}. \tag{15}$$

Let us now examine the solutions of Eq. (2) when (i) Eq. (13) is violated and (ii) when Eq. (13) is satisfied, but x lies outside the range specified by Eq. (15). The experimentalist should find this examination of value since it will determine (i) whether to expect waves in the x direction at all in plasmas having density gradients steep

enough to violate the WKB criterion and (ii) whether to expect waves in the regions where, according to Eq. (15), the WKB method is invalid even for plasmas having weak density gradients.

For both of these cases we find it useful to change the independent variable of Eq. (2) to w, yielding

$$w\frac{d}{dw}\left((1-w)w\frac{dE_z}{dw}\right)-(k_zL)^2\left(1-\frac{w}{\beta}\right)E_z=0. \quad (16)$$

For the case where Eq. (13) is violated, we make the following transformation in Eq. (16):

$$E_z(w)=u(w)/[w(1-w)]^{1/2}, \quad (17)$$

where $u(w)$ satisfies the equation

$$\frac{d^2u}{dw^2}+\left(\frac{[1-(2k_zL)^2]+[(2k_zL)^2/\beta]w(1-w)}{[2w(1-w)]^2}\right)u=0. \quad (18)$$

We will only investigate the case where Eq. (13) is severely violated so that $(k_zL)^2/\beta \ll 1$. In this case, Eq. (18) becomes

$$\frac{d^2u}{dw^2}+\frac{1}{[2w(1-w)]^2}u=0, \quad (19)$$

which has the solution

$$u=C_1[w(1-w)]^{1/2}+C_2[w(1-w)]^{1/2}\ln[w(1-w)]^{1/2}, \quad (20)$$

where C_1 and C_2 are constants. This solution is clearly nonoscillatory. Therefore, when $k_zL \ll \beta^{1/2}$, a plasma having an exponential density profile has *no waves* in the x direction.

Let us now consider the solution of Eq. (2) when Eq. (13) is satisfied but when x lies outside the range specified by Eq. (15). From Eq. (14) we see that this situation occurs when $0 < w < \beta/(2k_zL)^2$ and when $1-\beta/(2k_zL)^2 < w < 1$. Since Eq. (13) is satisfied, the former inequality corresponds to $w \simeq 0$ (i.e., when x is near the point where $\omega_{pe}^2=\omega^2$), while the second corresponds to $w \simeq 1$ (i.e., when x is near the lower hybrid layer).

In the former case Eq. (16) may be approximated by an equation whose solution is

$$E_z(w)=H_{2k_zL}^{(2)}\left(\frac{2k_zL}{\beta^{1/2}}w^{1/2}\right), \quad (21)$$

where the Hankel function of the second kind has been chosen so that the direction of increasing phase agrees with that of the WKB solution. In the region of validity of Eq. (21) $[0 < w < \beta/(2k_zL)^2]$ the argument of the Hankel function ranges from 0 to 1, so that there is less than one wavelength in this region.

In the second case Eq. (16) may be approximated to an equation whose solution is

$$E_z(w)=H_0^{(1)}\left(\frac{2k_zL}{\beta^{1/2}}(1-w)^{1/2}\right). \quad (22)$$

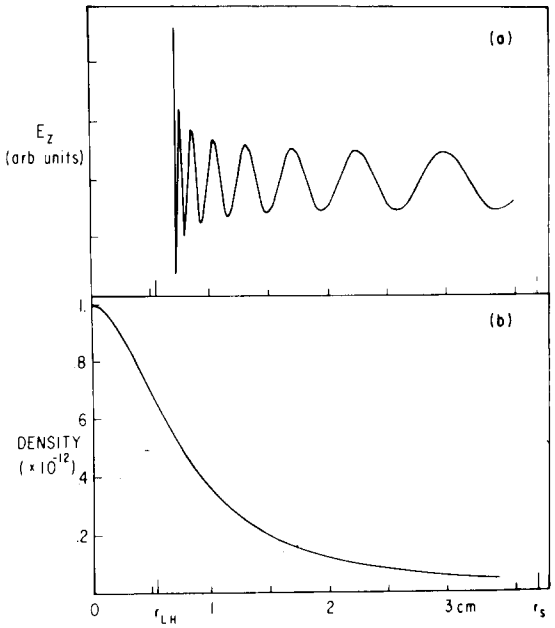

FIG. 2. (a) Numerical integration of the cylindrical version of Eq. (2); $2\pi/k_z = 33.3$ cm; $f = 50$ MHz; $B = 2$ kG; He gas. (b) Lorentzian density profile used in Fig. 2(a); $n(r) = 10^{12}\cdot(1+(r/0.75)^2)^{-1}$, where r is position in cm from the plasma center.

Again, the Hankel function argument varies between 0 and 1, so that there is also less than one wavelength in this region.

We summarize our results concerning inhomogeneous plasmas:

1. When $(k_zL)^2 \ll (m_e/m_i)(1-\omega^2/|\omega_{ci}\omega_{ce}|)$, there are no waves between the source and the lower hybrid layer.

2. When $(k_zL)^2 \gg (m_e/m_i)(1-\omega^2/|\omega_{ci}\omega_{ce}|)$, there are waves as given by the WKB solution, Eq. (5), but only in the region specified by Eq. (15). Outside of this region, i.e., near where $K_{xx}=0$ and near where $K_{zz}=0$, there is less than a wavelength as shown in the discussions after Eq. (21) and (22). In the remainder of the paper we will assume the above arguments to be valid for arbitrary density profiles, with L taken as a local e-folding scale length. We will also assume that the density profile always satisfies Eq. (13), so that we may use the WKB method in the region specified by Eq. (15).

Before leaving this section, in Fig. 2 we present some numerical solutions of Eq. (2) for a typical laboratory plasma density profile. From this figure we see qualitative agreement with the foregoing discussions. We note that there are a finite number of wavelengths between the hybrid layer and the plasma boundary.

III. COLD PLASMA WAVES GENERATED BY A FINITE STRUCTURE

Using the WKB method, let us now consider the effect of a spatially finite rf exciting structure upon the propagation of lower hybrid waves. However, a difficulty arises because a finite source generates a broad k_z spectrum. From the arguments of the preceding section, and in particular from Eq. (15), we see that the domains of WKB validity are different for the different k_z modes generated by the finite source. In order to have the same domain for all the

modes, we define

$$\epsilon = \beta[4(k_{z(\min)}L)^2]^{-1} \tag{23}$$

and

$$x_0 = x_1 - 2L\ln(2k_{z(\min)}L)^{-1}, \tag{24}$$

where $k_{z(\min)}$ is the smallest k_z generated by the source, and typically, $k_{z(\min)} \simeq \pi/a$ with a being the length of the source. When $\epsilon < x < x_0$, Eq. (15) is satisfied for all the k_z modes generated by the source (see Fig. 1).

The WKB solution is invalid in the region $x_0 < x < x_s$, where x_s is the position of the source (see Fig. 1). In principle, the solution in this region may be found. For example, for an exponential density profile the solution may be obtained by superimposing the Hankel functions of Eq. (21), weighted according to the k_z spectrum of the source. However, for arbitrary density profiles, this approach is not very tractable. Instead, since $|x_0 - x_s|$ is very small, we will assume that the total E_z field at x_0 resulting from the summation of all the k_z modes is approximately proportional to the field at the rf structure. In Appendix A we show that this assumption artificially introduces the singularities in the cones of Refs. 3–5 and that in a more accurate analysis the singularities would be replaced by peaks inversely proportional to $|x_s - x_1|$. Let us now proceed assuming $E_z(x_0, z) \propto E_z(x_s, z)$, but realizing the limitations of this assumption.

The amplitude at $x = x_0$ of each k_z mode excited by the structure is

$$E_z(x_0, k_z) = \frac{1}{2\pi}\int_{-\infty}^{\infty} dz'\, E_z(x_0, z')\exp(-ik_z z'). \tag{25}$$

Each k_z mode propagates according to the WKB solution given in Eq. (5). The solution for the field of a finite structure is found by using Eq. (25) for the amplitude of each k_z mode in Eq. (5), and then integrating over all k_z to give

$$E_z(x, z) = \frac{A(x, x_0)}{2\pi i}\int_{-\infty}^{\infty} dz'\, E_z(x_0, z') \times \left\{P\frac{1}{z - z' - g(x)} - P\frac{1}{z - z' + g(x)} + i\pi\delta[z - z' - g(x)] + i\pi\delta[z - z' + g(x)]\right\}, \tag{26}$$

where P designates the principal value and δ is the Dirac delta function. Convergence of the integrals at $k_z = \pm\infty$ has been assured by assuming that g has a small positive imaginary component. This would appear explicitly if collisions had been included in the dielectric tensor. The wave is nearly electrostatic since $ck_z/\omega \gg 1$, so that the same equation holds for $\phi(x, z)$ where $E_z = -\partial\phi/\partial z$.

The form of Eq. (26) shows that the potential in the region $x < x_0$ is connected to the potential at x_0 by the characteristics $z = \pm g(x)$. This is an immediate consequence of the fact that in this region the partial differential equation Eq. (A1) is hyperbolic and has solutions propagating along the above-mentioned characteristics. The potential in the plasma will be nonzero only at points that can be connected by these characteristics to points on the line $x = x_0$ having nonzero potential. In Appendix A we show: (1) that our assumption $E_z(x_0, z) \propto E_z(x_s, z)$ allows the existence of singular potentials on the line $x = x_0$, and hence singular potentials in the region $x < x_0$; and (2) that a more correct analysis would lead to bounded potentials on the line $x = x_0$, and hence bounded potentials in the region $x < x_0$.

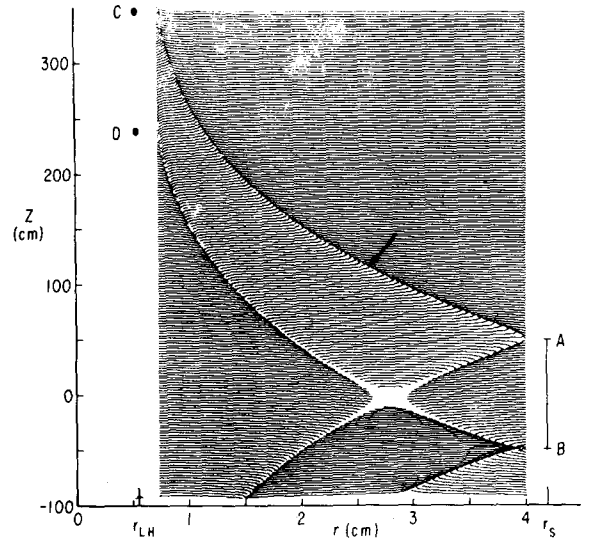

FIG. 3. Plots of potential generated by a 100 cm long parallel plate rf source. The plates are located along the line AB. The density profile is as given in Fig. 2(b); $f = 50$ MHz; $B = 2$ kG; He gas. Divergent points of the potential are shown as blanks (arrow). The hot plasma wave field (not shown) consists of singularities which start at C and D, and extend to the right.

The field in the plasma will now be calculated for two possible rf structures, one consisting of a metal plate parallel to the z axis, the other a slow wave structure.[6,7] For the parallel plate $\phi(x_0, z) = 1$ when $|z| \leq a$, and $\phi(x_0, z) = 0$ when $|z| > a$. Using Eq. (26) the potential in the plasma is found to be

$$\phi(x, z) = \frac{1}{2\pi i}A(x, x_0)\left[\ln\left(\frac{(a + z - g)}{(a - z + g)}\cdot\frac{(a - z - g)}{(a + z + g)}\right) + i\pi[\Theta(a - |z - g|) + \Theta(a - |z + g|)]\right], \tag{27}$$

where Θ is the Heaviside function. Using the fact that $\ln(-|x|) = \ln|x| + i\pi$, we split the logarithmic term of ϕ into its real and imaginary parts, Reϕ and Imϕ. Imϕ is shown in Fig. 3. A slab plasma with the density shown in Fig. 2(b) has been used for this calculation; r is the distance to the center of the plasma, and x is the distance to the lower hybrid layer. The rf source is at r_s and the lower hybrid layer is at r_{LH}. Imϕ has singularities on the cones $z = \pm a \pm g(x)$; since $g(x_0) = 0$, these cones emanate from the ends of the plates at $z = \pm a$. From the arguments of Appendix A we realize that these singularities result from the artificial assumption $E_z(x_0, z) \propto E_z(x_s, z)$ and that an exact solution would have finite peaks rather than singularities. In addition, we note that because these peaks are sharp, their Fourier transform contains high k_z modes for which the cold plasma analysis used here is inappropriate.

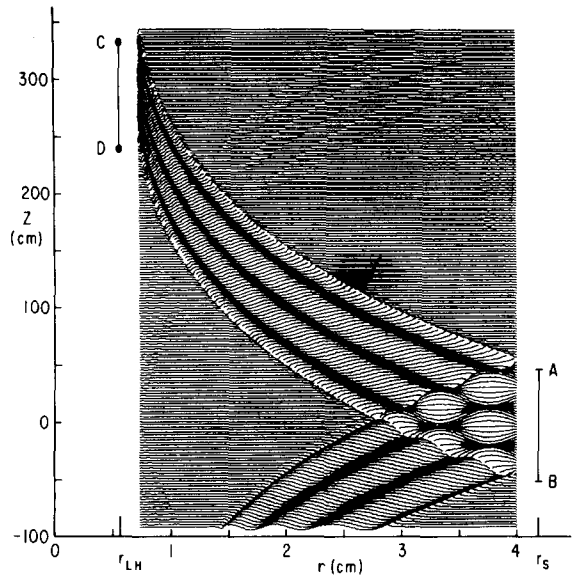

FIG. 4. Plots of electric field generated by a 100 cm long slow wave structure (located along line AB). $2\pi/k_z = 33.3$ cm; density profile as in Fig. 2(b) $f = 50$ MHz, $B = 2$ kG, He gas. Sharp logarithmic singularities shown as blanks (arrow) bound the wave field. The hot plasma wave field (not shown) starts from the line CD and extends to the right.

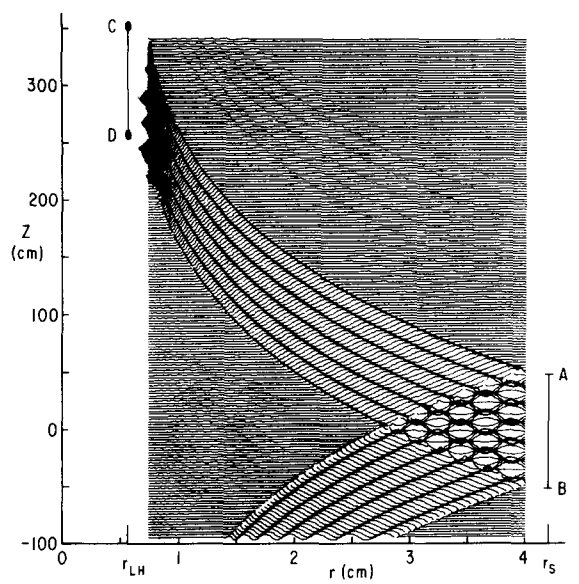

FIG. 5. Same parameters as in Fig. 4, except that $2\pi/k_z = 16.6$ cm.

A hot plasma analysis would predict severe Landau damping of modes having $k_z \gtrsim \omega/v_{Te}$, where v_{Te} is the electron thermal velocity. This would destroy the sharpness of the cones as they penetrated the plasma.[5]

Taking into account the Heaviside functions implicit in the logarithmic term of Eq. (27), we find

$$\mathrm{Re}\phi(x, z) = \tfrac{1}{2}A(x, x_0)\left\{1 - \Theta\left[\frac{(a+z-g)}{(a-z+g)} \times \frac{(a-z-g)}{(a+z+g)}\right] + \Theta(a - |z-g|) + \Theta(a - |z+g|)\right\}. \quad (28)$$

The cones $z = \pm a \pm g(x)$ divide the xz plane of Fig. 3 into six regions. By evaluating the Heaviside functions of Eq. (28) in these regions we find: $\mathrm{Re}\phi = A(x, x_0)$ in the triangular region immediately to the left of the line AB; $\mathrm{Re}\phi = A(x, x_0)/2$ in the region (excepting the triangle) between the two cones starting at A and B and going to C and D, and also in a similar region between the cones starting at A and B and going in the negative z direction; $\mathrm{Re}\phi = 0$ in the remaining regions. Thus, $\mathrm{Re}\phi$ is essentially an image of the potential along the source at AB, propagating between the two pairs of cones. In the triangular region the signals going in the positive and negative z directions overlap.

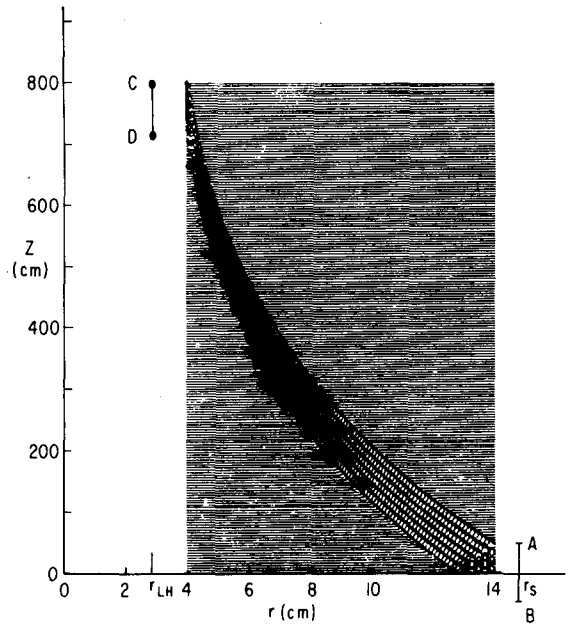

FIG. 6. Plots of electric field generated by a 100 cm long slow wave structure in a "tokamak-like" plasma. Density $n(r) = 10^{14} \times (1 + (r/5)^2)^{-1}$; $2\pi/k_z = 15$ cm; $f = 1$ GHz; $B = 40$ kG; deuterium gas. Hot plasma field (not shown) starts from the line CD and extends to the right.

For the slow wave structure $\phi(x_0, z) = \cos k_0 z$ when $|z| \leq a$, and $\phi(x_0, z) = 0$ when $|z| > a$. Here, a definite k_z has been imposed, so that a definite k_x is to be expected. By using Eq. (26), the solution for the structure is found to be

$$\begin{aligned}\phi(x, z) = {} & [A(x, x_0)/2\pi i](-\cos[k_0(z-g)] \\ & \times \{\mathrm{Ci}[k_0(a-z+g)] - \mathrm{Ci}[k_0(a+z-g)]\} \\ & + \sin[k_0(z-g)]\{\mathrm{Si}[k_0(a-z+g)] \\ & + \mathrm{Si}[k_0(a+z-g)]\} + \cos[k_0(z+g)] \\ & \times \{\mathrm{Ci}[k_0(a-z-g)] - \mathrm{Ci}[k_0(a+z+g)]\} \\ & - \sin[k_0(z+g)]\{\mathrm{Si}[k_0(a-z-g)] \\ & + \mathrm{Si}[k_0(a+z+g)]\} + i\pi \cos[k_0(z-g)] \\ & \times \Theta(a - |z-g|) + i\pi \cos[k_0(z+g)] \\ & \times \Theta(a - |z+g|)), \end{aligned} \quad (29)$$

where Si and Ci are the sine and cosine integrals (Ref. 10, p. 231). Figures 4–6 show numerical plots obtained from the imaginary part of Eq. (29) for finite k_0 and finite a. Parameters typical of a small plasma device were used for Figs. 4 and 5, and typical tokamak parameters were used for Fig. 6. The field from the slow wave structure consists

of waves bounded by cones coming from the ends. A comparison of Figs. 4 and 5 shows that the number of wavelengths existing in the x direction is $2k_0a$, which is the number of wavelengths in the z direction along the slow wave structure. The field in the x direction near the resonant layer is really a reduced image of the field applied in the z direction. The total distance the cone travels in the z direction is $g(0)$ which is the order of $(m_i/m_e)^{1/2}x_s$. Thus, in a tokamak the cone might circle the torus before reaching the resonant layer (see Fig. 6). In such situations the importance of toroidal effects upon wave propagation must be examined.

In the limit $k_0 \to 0$, Eq. (29) should give the parallel plate solution given by Eq. (27). In the limit $W \to 0$, $\mathrm{Si}(W) \to 0$, and $\mathrm{Ci}(W) \to \ln W$ so that the solution given by Eq. (29) does indeed revert to the parallel plate solution when $k_0 \to 0$ (Ref. 10, p. 231). In the limit $a \to \infty$, $\mathrm{Si} \to \pi/2$ and the Ci's cancel, so that we obtain

$$\lim_{a\to\infty} \phi(x, z) = A(x, x_0)\tfrac{1}{2}\{\exp[-ik_0(z - g)] + \exp[ik_0(z + g)]\}. \tag{30}$$

Inserting the time dependence $\exp(-i\omega t)$ and taking the real part yields propagating waves:

$$\lim_{a\to\infty} \phi(x, z, t) = A(x, x_0)\cos(k_0 z)\cos[k_0 g(x) - \omega t]. \tag{31}$$

Thus, in order to verify experimentally the cold plasma dispersion relation Eq. (4), it is necessary to impose phase variations in the z direction at $x = x_0$. In addition, one must supply as many waves in the z direction at x_0 as one hopes to see in the x direction (see Figs. 4 and 5).

IV. REVIEW OF LINEARLY CONVERTED HOT PLASMA WAVES

Stix has shown that it is necessary to include thermal effects when K_{xx} vanishes.[1] Here, we shall review this calculation before extending it in Secs. V and VI to include effects of collisions and a finite source. With the inclusion of thermal effects Eq. (2) becomes

$$\frac{d}{dx}\left[\left(\alpha\frac{d^2}{dx^2} + K_{xx}\right)\frac{dE_z}{dx}\right] - k_z^2 K_{zz}E_z = 0, \tag{32}$$

where

$$\alpha = \sum_{\sigma=i,e} \frac{3\omega_{p\sigma}^2 \kappa T_\sigma/m_\sigma}{(\omega^2 - \omega_{c\sigma}^2)(\omega^2 - 4\omega_{c\sigma}^2)} \simeq \frac{3\omega_{pi}^2}{\omega^4}\frac{\kappa T_i}{m_i} + \frac{3}{4}\frac{\omega_{pe}^2}{\omega_{ce}^4}\frac{\kappa T_e}{m_e}, \tag{33}$$

where T_σ is the temperature, σ designates ions or electrons, and κ is Boltzman's constant.[1,11] For x sufficiently small that

$$|\tfrac{1}{2}x^2 K_{xx}''(0)| \ll |xK_{xx}'(0)|, \tag{34}$$

it is accurate to write $K_{xx}(x) \cong xK_{xx}'(0)$. We note that Eq. (34) is satisfied when $x \ll L$ and also that $K_{xx}'(0) \sim L^{-1}$, where L is the scale length near the hybrid layer. When Eq. (34) is satisfied, it is accurate to rewrite Eq. (32) in the form

$$\alpha\frac{d^4E_z}{dx^4} + \frac{d\alpha}{dx}\frac{d^3E_z}{dx^3} + xK_{xx}'\frac{d^2E_z}{dx^2} + K_{xx}'\frac{dE_z}{dx} - k_z^2K_{zz}E_z = 0, \tag{35}$$

where a prime means derivative with respect to x at $x = 0$. The fourth term which was omitted in Ref. 1 is of importance in the amplitude of the solutions. By transforming to dimensionless variables,

$$\xi = \alpha^{-1/3}(K_{xx}')^{1/3}x, \qquad \mu = -k_z^2\alpha^{1/3}(K_{xx}')^{-4/3}K_{zz},$$
$$b = \frac{1}{\alpha}\frac{d\alpha}{d\xi}, \tag{36}$$

Eq. (35) becomes

$$\frac{d^4E_z}{d\xi^4} + b\frac{d^3E_z}{d\xi^3} + \xi\frac{d^2E_z}{d\xi^2} + \frac{dE_z}{d\xi} + \mu E_z = 0. \tag{37}$$

The second term may be dropped since $b \sim (\lambda/L)^{2/3} \ll 1$ where λ is the order of the Debye length or the Larmor radius, depending on which term dominates in Eq. (33). By Laplace transforming Eq. (37) a first-order equation for the Laplace transform of E_z is obtained. The inverse Laplace transform of the solution of this first-order equation is

$$E_z(x, k_z) = (2\pi i)^{-1}\int_C dp\,\exp(\tfrac{1}{3}p^3 - \mu/p + \xi p - \ln p). \tag{38}$$

Figure 7 shows how the path C in the complex P plane is chosen so that (i) for $\xi < 0$ it may be deformed to pass through saddle points giving evanescent solutions and (ii) for $\xi > 0$ it may be deformed to pass through the saddle point corresponding to the cold wave generated by the rf source and *not* through the saddle point corresponding to an incoming hot plasma wave. This last requirement forces C to be chosen so that for $\xi > 0$ it may be deformed to pass through the saddle point corresponding to an outgoing hot plasma wave.[1] The direction of propagation is taken to be that of the group velocity which for the cold plasma wave is opposite to the phase velocity. For the hot plasma wave the group velocity is in the same direction as the phase velocity. The joining condition between the approximate saddle point solutions for $\xi > 0$ and $\xi > 0$, valid for $\xi^2 \gg |\mu| \gg |1/\xi|$, is[1]

$$\frac{-\exp(-\frac{2}{3}|\xi|^{3/2})}{|\xi|^{3/4}} + \frac{1}{i^{1/2}}\frac{\exp[-2(\mu|\xi|)^{1/2}]}{(-|\xi|\mu)^{1/4}} \leftrightarrow \frac{-\exp[\frac{2}{3}(i\xi)^{3/2}]}{i^{3/2}\xi^{3/4}} + \frac{1}{i^{1/2}}\frac{\exp[2i(\mu\xi)^{1/2}]}{(\xi\mu)^{1/4}}. \tag{39}$$

The minus sign appears in front of the hot plasma wave solution because the integration path passes through the saddle point in the direction opposite to the conventional one (see Fig. 7).

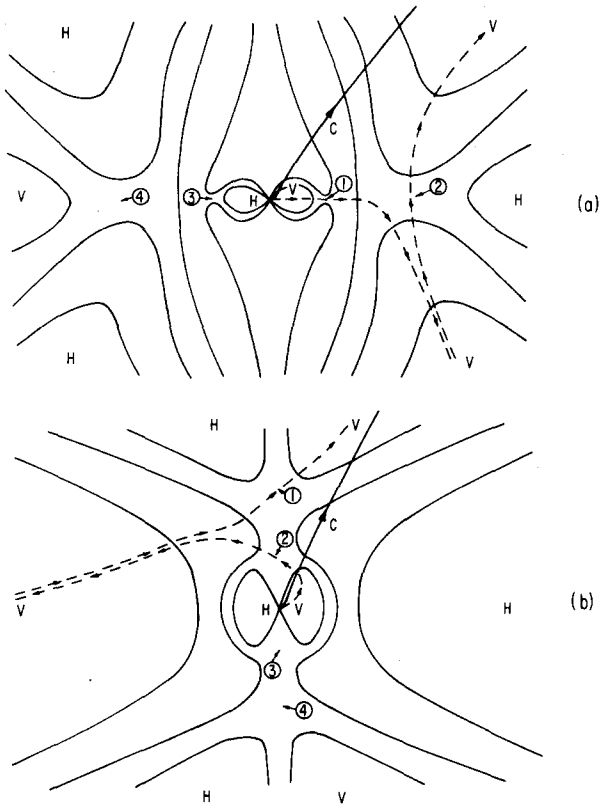

FIG. 7. Contour path C used for the evaluation of Eq. (29). A unique C is found by requiring that it satisfy all four boundary conditions given in requirements (i) and (ii) in text after Eq. (29). (a) shows location of saddle points for $\xi < 0$; saddle points 1, 2, 3, 4 give cold evanescent, hot evanescent, cold growing, and hot growing waves, respectively; H and V signify hills and valleys. (b) shows contours for $\xi > 0$; saddle points 1, 2, 3, 4, give hot outgoing, cold ingoing, cold outgoing, and hot ingoing waves, respectively. Dotted curves are allowed deformations of C.

Using Eq. (36) the condition $\xi^2 \gg |\mu| \gg |1/\xi|$ becomes

$$\left|\frac{K_{xx}'x^3}{\alpha}\right| \gg \left|k_z^2\frac{K_{xx}x}{K_{xx}'}\right| \gg 1. \tag{40}$$

The first two terms above are approximately the squares of the respective phases of the hot and cold plasma waves. The inequality Eq. (34) used for the derivation of Eq. (35) requires that $x \ll L$. This condition implies that in order for a region where Eq. (40) is satisfied to exist we must have $(k_zL)^2 |K_{zz}(0)| \gg 1$ and $k_z^2\alpha |K_{zz}(0)| \ll 1$. These conditions are easily satisfied for typical plasma parameters.

We note from Eq. (40) that the region where Eq. (39) is valid moves toward larger values of $|x|$ with increasing k_z.[12]

Since Eq. (32) is a linear equation, its approximate solutions given by Eq. (39) may be multiplied by any constant. By substituting for ξ and μ and multiplying by the constant $(i|k_z|K_{xx}')^{1/2}$ the right-hand side of Eq. (39) becomes

$$\begin{aligned} E_z(x, z) &= i|k_z|^{1/2}\left(\frac{\alpha}{(xK_{xx}')^3}\right)^{1/4} \\ &\times \exp[2/3i\alpha^{-1/2}(K_{xx}')^{1/2}x^{3/2}] \\ &+ (-xK_{xx}'K_{zz})^{-1/4}\exp\left[2i\left(\frac{-k_z^2xK_{zz}}{K_{xx}'}\right)^{1/2}\right]. \end{aligned} \tag{41}$$

When x satisfies Eq. (40), we have $xK_{xx}' = K_{xx}$, and the phases in Eq. (41) may be written as integrals so that

$$\begin{aligned} E_z(x, k_z) &= i|k_z|^{1/2}\left(\frac{\alpha}{K_{xx}^3}\right)^{1/4}\exp\left[i\int_0^x\left(\frac{K_{xx}}{\alpha}\right)^{1/2}dx'\right] \\ &+ (-K_{xx}K_{zz})^{-1/4} \\ &\times \exp\left[i|k_z|\int_0^x\left(\frac{-K_{zz}}{K_{xx}}\right)^{1/2}dx'\right]. \end{aligned} \tag{42}$$

Except for a different amplitude factor, the second term in the above equation is formally the same as the WKB solution given by Eqs. (5), (6), and (7). However, the amplitude of the solution given by Eq. (42) is not yet determined. In order to make the second term of Eq. (42) correspond to the cold plasma WKB wave coming from the source [given by Eq. (5)] we must multiply Eq. (42) by the constant $E_{zc}(x_0, k_z)[-K_{xx}(x_0)K_{zz}(x_0)]^{1/4}\exp[i|k_z|g(0)]$, where $E_{zc}(x_0, k_z)$ is the amplitude at x_0 of the k_z Fourier mode of the cold plasma wave given by Eq. (25). This yields

$$\begin{aligned} E_z(x, k_z) &= E_{zc}(x_0, k_z) \\ &\times \left\{i|k_z|^{1/2}[-K_{xx}(x_0)K_{zz}(x_0)]^{1/4}\left(\frac{\alpha}{K_{xx}^3}\right)^{1/4}\right. \\ &\times \exp\left[i\int_0^x\left(\frac{K_{xx}}{\alpha}\right)^{1/2}dx' + i|k_z|g(0)\right] \\ &\left.+\left(\frac{K_{xx}(x_0)K_{zz}(x_0)}{K_{xx}(x)K_{zz}(x)}\right)^{1/4}\exp[i|k_z|g(x)]\right\}. \end{aligned} \tag{43}$$

The hot plasma wave term contains the factor $\exp[i|k_z|g(0)]$ which is formally like $\exp[-ik_x(x_0 - 0)]$. This type of factor occurs in a Fourier amplitude when a coordinate transformation has been made in real space. In this case the transformation comes about because $x = x_0$ was used as the origin for the solution of Eq. (2), whereas $x = 0$ was the origin used in the solution of Eq. (32). This factor explicitly contains k_z; physically this means that the origin of the hot plasma wave is also shifted in the z direction to the position where the cold plasma wave reached the resonant layer (see Figs. 4, 5, 6).

V. COLLISIONAL EFFECTS

The inclusion of collisions changes K_{xx} to $K_{xx} + i\delta K_{xx}$ and K_{zz} to $K_{zz} + i\delta K_{zz}$, where the imaginary terms are proportional to the ion and electron collision frequencies, $\nu_{i,e}$. Here, we shall assume that $\nu_{i,e}/\omega \ll 1$ so that with the exception of the region near the lower hybrid layer, $\delta K_{xx} < K_{xx}$ and $\delta K_{zz} < K_{zz}$. At the hybrid layer K_{xx} vanishes while δK_{xx} is finite. Thus, we expect most of the attenuation due to collisions to come from near the lower hybrid layer. Since $\delta K_{zz} \ll K_{zz}$ throughout the range of interest, δK_{zz} introduces much less attenuation than δK_{xx}. With the inclusion of δK_{xx} and δK_{zz} the new form of Eq. (37) is obtained by the substitution $\xi \to \xi + id$ and $\mu \to \mu + i\delta\mu$, where d and $\delta\mu$ are proportional to collision frequencies. Since the only effect of this substitution is to shift slightly the positions of the saddle points of Eq. (38), the new forms of Eqs. (39) and (41) are also obtained by making

the same substitution. The transformation from Eq. (41) to Eq. (42) will have the same formal result as before, except that K_{xx} is replaced by $K_{xx} + i\delta K_{xx}$ and K_{zz} is replaced by $K_{zz} + i\delta K_{zz}$. This gives the important result that the hot plasma wave amplitude contains the factor $\exp[+i \mid k_z \mid g(0)]$, where $g(0)$ is complex and is calculated using $K_{xx} + i\delta K_{xx}$ and $K_{zz} + i\delta K_{zz}$. This means that the net amplitude of the hot plasma wave is reduced by the damping factor $\exp(-D)$ where

$$D = \mathrm{Im} \int_{x_0}^{0} \mid k_z \mid \left(\frac{-(K_{zz} + i\delta K_{zz})}{(K_{xx} + i\delta K_{xx})}\right)^{1/2} dx. \tag{44}$$

The factor $\exp(-D)$ is clearly the damping experienced by the cold plasma wave propagating from $x = x_0$ to $x = 0$. Since the cold plasma wave effectively generates the hot plasma wave at the resonant layer, it is reasonable that damping of the cold plasma wave on its way to the resonant layer produces a hot plasma wave of correspondingly reduced amplitude. Equation (44) is evaluated in Appendix B to give

$$D \simeq \mid k_z \mid L[-2K_{zz}(0)\delta K_{xx}]^{1/2}. \tag{45}$$

From Eqs. (1) and (9) $-K_{zz}(0) \sim \beta^{-1}$ so that $D \gtrsim 1$ if

$$\delta K_{xx} \gtrsim \tfrac{1}{2}\beta/(k_z L)^2. \tag{46}$$

Since $\beta < m_e/m_i$ and $\delta K_{xx} \sim 2(\nu_i + \nu_e)/\omega$, the factor $\exp(-D)$ may be quite small even for a plasma with low collision frequency. When $\exp(-D)$ is small, the cold plasma wave dissipates its energy by means of collisional effects near the lower hybrid layer instead of converting into a hot plasma wave. For the plasma parameters given in the caption of Fig. 4 (a typical small scale experiment) collisional effects predominate over mode conversion if $(\nu_i + \nu_e)/\omega > 10^{-5}$. Since in typical small-scale devices $\nu_e/\omega \simeq 10^{-2} - 10^{-3}$, mode conversion will be difficult to observe in these devices, unless great care is taken to optimize experimental parameters. For the plasma parameters given in the caption of Fig. 6 (tokamak conditions), collisional effects predominate over mode conversion if $(\nu_i + \nu_e)/\omega > 5 \times 10^{-4}$. Since in typical tokamaks $\nu_e/\omega \simeq 10^{-5}$, we conclude that mode conversion will dominate.

VI. HOT PLASMA WAVES EXCITED BY A FINITE SOURCE

From the form of the linear mode conversion given by Eq. (43), it is clear that each incoming cold plasma mode $\exp(ik_z z)$ excites a corresponding hot plasma mode. A finite source will excite a whole spectrum of k_z modes each of which converts linearly to a hot plasma mode according to Eq. (43). The Fourier amplitude $E_z(x_0, k_z)$ occurring in Eq. (43) is thus the same Fourier transform of the cold plasma wave existing at x_0, given by Eq. (25). The fact that this Fourier amplitude is also a factor of the hot plasma wave reflects the one-to-one correspondence between an incoming cold plasma mode and an outgoing hot plasma mode with the same z dependence. The hot plasma wave field, $E_{zh}(x, z)$, found from the inverse Fourier transform of the first term of Eq. (43) is given by

$$E_{zh}(x, z) = \int dk_z \left\{E_{zc}(x_0, k_z) i \mid k_z \mid^{1/2} \left(\frac{-K_{xx}(x_0)K_{zz}(x_0)\alpha}{K_{xx}^3(x)}\right)^{1/4} \times \exp\left[i\int_0^x \left(\frac{K_{xx}}{\alpha}\right)^{1/2} dx' + i \mid k_z \mid g(0) + ik_z z\right]\right\}. \tag{47}$$

After substituting Eq. (25) for $E_{zc}(x_0, k_z)$ and then reversing the order of the k_z and z' integrations, Eq. (47) becomes

$$E_{zh}(x, z) = \left(\frac{-K_{xx}(x_0)K_{zz}(x_0)\alpha}{K_{xx}^3(x)}\right)^{1/4} \times \exp\left[i\int_0^x \left(\frac{K_{xx}}{\alpha}\right)^{1/2} dx'\right] \times \int_{-\infty}^{\infty} dz' \left[E_{zc}(x_0, z') \int_{-\infty}^{\infty} \frac{dk_z}{2\pi} i \mid k_z \mid^{1/2} \times \exp[ik_z(z - z') + i \mid k_z \mid g(0)]\right]. \tag{48}$$

By using the relation (Ref. 10, p. 255)

$$\Gamma(y) = W^y \int_0^\infty t^{y-1} \exp(-Wt\, dt), \tag{49}$$

$$\mathrm{Re}y > 0, \qquad \mathrm{Re}w > 0,$$

the k_z integral in Eq. (48) may be evaluated, and we obtain

$$E_{zh}(x, z) = \chi(x) \frac{\exp[i(3\pi/4)]}{4\pi^{1/2}} \int_{-\infty}^{\infty} dz'\, E_{zc}(x_0, z') \times \left(\frac{1}{[-z' + z + g(0)]^{3/2}} + \frac{1}{[z' - z + g(0)]^{3/2}}\right), \tag{50}$$

where

$$\chi(x) = i\left(\frac{-K_{xx}(x_0)K_{zz}(x_0)\alpha}{K_{xx}^3(x)}\right)^{1/4} \exp\left[i\int_0^x \left(\frac{K_{xx}}{\alpha}\right)^{1/2} dx'\right]. \tag{51}$$

We have evaluated Eq. (50) for parallel plates and for a slow wave source. It should be noted that the x dependence factors out as $\chi(x)$, so that the wave trajectory is not conical as it was for the cold plasma wave.

For parallel plates, by again assuming that $E_z = -\partial\phi/\partial z$, $\phi(x_0, z) = 1$ for $\mid z \mid \leq a$, and $\phi(x_0, z) = 0$ for $\mid z \mid > a$, Eq. (50) gives

$$\phi(x, z) = -\chi(x) \frac{\exp(i3\pi/4)}{2\pi^{1/2}} \left(\frac{1}{[a + z + g(0)]^{1/2}} - \frac{1}{[-a + z + g(0)]^{1/2}} + \frac{1}{[a - z + g(0)]^{1/2}} - \frac{1}{[-a - z + g(0)]^{1/2}}\right). \tag{52}$$

Thus, starting from the points where the resonant cones have intercepted the lower hybrid layer, (at CD in Fig. 3) weak singularities propagate out in the x direction.

For the slow wave structure $E_z(x_0, z) = \cos k_{0z}$ when $|z| \leq a$ and $E_z(x_0, z) = 0$ when $|z| > a$, and Eq. (50) gives

$$
\begin{aligned}
E_{zh}(x, z) = -\chi(x) \exp\left(\frac{i3\pi}{4}\right)\frac{k_0^{1/2}}{2\pi^{1/2}}
&\times\left[\left(\frac{\cos(k_0 z')}{\{k_0[z' + g(0) + z]\}^{1/2}}\right)_{z'=-a}^{z'=a}\right.\\
&+\left(\frac{\cos(k_0 z')}{\{k_0[z' + g(0) - z]\}^{1/2}}\right)_{z'=-a}^{z'=a}\\
&+ (2\pi)^{1/2}[\cos\{k_0[g(0) + z]\}\\
&\times (S\{k_0[a + g(0) + z]\}\\
&- S\{k_0[-a + g(0) + z]\})\\
&- \sin\{k_0[g(0) + z]\}\\
&\times (C\{k_0[a + g(0) + z]\}\\
&- C\{k_0[-a + g(0) + z]\})\\
&+ \cos\{k_0[g(0) - z]\}(S\{k_0[a + g(0) - z]\}\\
&- S\{k_0[-a + g(0) - z]\})\\
&- \sin\{k_0[g(0) - z]\}(C\{k_0[a + g(0) - z]\}\\
&\left.- C\{k_0[-a + g(0) - z]\})\right], \qquad (53)
\end{aligned}
$$

where C and S are the Fresnel integrals (Ref. 10, p. 300). This field consists of waves in the x and z directions, bounded by singularities of the type given by Eq. (52).

The most significant difference between Eqs. (52) and (53) is that the field due to parallel plates is concentrated on the lines $x > 0$, $z = \pm a \pm g(0)$, while the field due to the slow-wave structure is evenly distributed in the regions between the pairs of lines $x > 0$, $z = \pm a + g(0)$ and $x > 0$, $z = \pm a - g(0)$. Thus, the slow wave structure generates a spatially more evenly distributed hot plasma wave than the parallel plate.

In the limit $k_0 \to 0$, $S \to 0$, and $C \to 0$ so that Eq. (52) is retrieved as it should be. For an infinitely long slow wave structure $a \to \infty$, and the first two terms of Eq. (53) vanish. By using the relations

$$
\begin{aligned}
&S(-x) = -iS(x),\\
&C(-x) = iC(x), \qquad (54)\\
&\lim_{x\to\infty} C(x) = \lim_{x\to\infty} S(x) = 1/2,
\end{aligned}
$$

Eq. (53) becomes

$$
\lim_{a\to\infty} E_{zh}(x, z) = \chi(x) k_0^{1/2} \exp[ik_0 g(0)] \cos(k_0 z). \qquad (55)
$$

By inserting the time dependence $\exp(-i\omega t)$, substituting for $\chi(x)$ and taking the real part, Eq. (55) becomes an outward propagating plane wave:

$$
\begin{aligned}
\lim_{a\to\infty} E_{zh}(x, z, t) = &-\left(\frac{-K_{xx}(x_0)K_{zz}(x_0)\alpha}{K_{xx}^3(x)}\right)^{1/4} k_0^{1/2}\cos(k_0 z)\\
&\times \sin\left\{\left[\int_0^x \left(\frac{K_{xx}}{\alpha}\right)^{1/2} dx' + k_0 g(0) - \omega t\right]\right\}. \qquad (56)
\end{aligned}
$$

If damping of the incoming cold plasma wave is included, then the above result must be multiplied by $\exp(-k_0 |\operatorname{Im} g(0)|)$ as shown in Sec. V.

VII. SUMMARY

We have found the local wavelength of lower hybrid waves for plasmas with such large density gradients that the WKB approximation is not valid. Such large density gradients are frequently found in laboratory plasmas, and in these situations the present theory should give a much better explanation of experimental results than the WKB theory. We have also examined, in detail, the propagation from a point near the plasma boundary to the lower hybrid layer of waves excited by a finite rf source. We have shown that a slow wave rf source having a field $\phi \sim \cos(k_0 z)$ generates cold plasma waves having well-defined wavelengths, whereas a parallel plate source having a field $\phi \sim$ const generates in the plasma only singular cones and an image of the source but no waves. We have applied some of these results to a tokamak-like plasma, and found that in typical present and near future devices microwave power injected at the outside periphery may require rather long axial distances (i.e., of the order of 10–30 m) for penetration to the lower hybrid layer.

We have shown quantitatively how collisional damping of the cold plasma wave in the region immediately before the lower hybrid resonant layer may absorb most of the energy of this wave before it has a chance to convert linearly to a hot plasma wave at the resonant layer. In particular, even weak collisions would cause a severe attenuation of the resulting converted hot plasma waves amplitude. Finally, we have shown that a parallel plate source generates hot plasma waves at the hybrid layer which are highly localized in the z direction, whereas a slow wave structure generates hot plasma waves evenly distributed in the z direction.

ACKNOWLEDGMENTS

One of the authors (P.B.) wishes to thank both Dr. M. N. Rosenbluth for discussions concerning the calculations of the collisional effects and Dr. M. D. Kruskal for discussions concerning the path deformation argument of the mode conversion calculation.

This work was supported by the U.S. Atomic Energy Commission Contract AT(11-1)-3073. One of the authors (P.B.) received financial support from the National Research Council of Canada in the form of a Post Graduate Fellowship.

APPENDIX A

To understand the limitations of the assumption $E_z(x_0, z) \propto E_z(x_s, z)$ used in Sec. III, let us consider the

partial differential equation

$$\frac{\partial}{\partial x} K_{xx} \frac{\partial E_z}{\partial x} + K_{zz} \frac{\partial^2}{\partial z^2} E_z = 0, \tag{A1}$$

from which Eq. (2) was derived. The region $x_0 < x < x_s$ is far from the lower hybrid layer so that, by using Eq. (1), Eq. (A1) in this region becomes approximately

$$\frac{\partial^2 E_z}{\partial x^2} + K_{zz} \frac{\partial^2 E_z}{\partial z^2} = 0. \tag{A2}$$

The most important feature of the region $x_0 < x < x_s$ is that K_{zz} changes sign in this region at $x = x_1$, the point where $\omega_{pe}^2 = \omega^2$. Equation (A2) is an elliptic partial differential equation when $x > x_1$ ($K_{zz} > 0$) and is a hyperbolic one when $x < x_1$ ($K_{zz} < 0$).

Solutions in the region $x > x_1$ will be analogous to those of the simplest elliptic equation, $\nabla^2\phi = 0$; in particular, two-dimensional point sources (line sources in three dimensions) will excite a field of equipotential surfaces concentric about the source and becoming singular at the source. Solutions in the region $x < x_1$ will be analogous to those of the simplest hyperbolic equation,

$$\frac{\partial^2\phi}{\partial t^2} = c^2 \frac{\partial^2\phi}{\partial x^2} \tag{A3}$$

except that here z replaces t. In particular, a two-dimensional point *disturbance* will propagate along characteristics in the x, z plane that are analogous to the characteristics $x \pm ct$ in the x, t plane of the simple wave equation.

The divergent fields in the plasma of Refs. 3–5 came about because the region $x_1 < x < x_s$ has been omitted, which is tantamount to assuming that the point source lies inside the region $x < x_1$ where disturbances propagate along characteristics. Since the potential at the source is singular, such an assumption will predict that a singularity propagates inside the plasma, which is nonphysical.

In reality, there must always be a low density region where $\omega_{pe}^2 < \omega^2$ between a physical source and the plasma so that there is always an "elliptic" region between the source and the "hyperbolic" region. In the "elliptic" region the potential is finite at any finite distance from the source. Thus, since $|x_s - x_1|$ is finite, the potential penetrating the "hyperbolic" region at the elliptic–hyperbolic interface is finite and the resulting potential propagating along the characteristics is finite.

It is clear that the maximum potential in the plasma will depend inversely on $|x_s - x_1|$ since the potential drops in this manner in the "elliptic" region and then propagates more or less without attenuation in the "hyperbolic" region. Thus, we may use the assumption $E_z(x_0, z) \propto E_z(x_s, z)$, but we must bear in mind that this will lead to artificial singularities in the plasma. We expect that by using a correct analysis the singularities would be replaced by peaks having an amplitude inversely proportional to $|x_s - x_1|$.

APPENDIX B: EVALUATION OF EQ. (35)

Near the lower hybrid layer we may write $K_{xx} = 1 - \exp(-x/L)$, where $x = 0$ is the position of the lower hybrid layer and L is the density e-folding scale length. We choose Δ to be the maximum value of x for which the approximation $K_{xx} \cong xK_{xx}'$ is valid. Evaluation of K_{xx}' and K_{xx}'' shows that $\Delta \lesssim L$. Since the attenuation experienced by the wave between $x = x_0$ and $x = 0$ is cumulative and since the main contribution to the integral in Eq. (44) comes from the region where K_{xx} becomes small, we may write

$$D > \mathrm{Im} \int_\Delta^0 |k_z| \left(- \frac{(K_{zz} + i\delta K_{zz})}{(K_{xx} + i\delta K_{xx})} \right)^{1/2} dx. \tag{B1}$$

The contributions of δK_{xx} and δK_{zz} to the damping are additive so that we may neglect the small effect of δK_{zz} without affecting the inequality in Eq. (B1). Using the fact that in the interval $0 \leq x \leq \Delta$, K_{zz} and δK_{xx} are approximately constant while $K_{xx} = xK_{xx}'$ we find on evaluating the integral in Eq. (B1) that

$$D \geq \mathrm{Im} \left\{ 2 |k_z| \left(\frac{-K_{zz}(0)\Delta}{K_{xx}'} \right)^{1/2} \left[\left(\frac{i\delta K_{xx}}{\Delta K_{xx}'} \right)^{1/2} - \left(1 + \frac{i\delta K_{xx}}{\Delta K_{xx}'} \right)^{1/2} \right] \right\}. \tag{B2}$$

Since $\Delta \lesssim L$, $\Delta K_{xx}' \sim 1$, and $\delta K_{xx}/(\Delta K_{xx}') \ll 1$. The square root of $\delta K_{xx}/(\Delta K_{xx}')$ is thus much larger than itself so that the first term on the right-hand side of Eq. (B2) dominates the other terms with the result that

$$D \gtrsim (|k_z|/K_{xx}')[-2K_{zz}(0)\delta K_{xx}]^{1/2}. \tag{B3}$$

Using the fact that $K_{xx}' \sim L^{-1}$, we obtain Eq. (45).

[1] T. H. Stix, Phys. Rev. Lett. **15,** 878 (1965).
[2] T. H. Stix, *The Theory of Plasma Waves* (McGraw-Hill, New York, 1962), Chap. 2.
[3] H. H. Kuehl, Phys. Fluids **5,** 1095 (1962).
[4] R. K. Fisher and R. W. Gould, Phys. Fluids **14,** 857 (1971).
[5] R. J. Briggs and R. R. Parker, Phys. Rev. Lett. **29,** 852 (1972).
[6] W. M. Hooke and S. Bernabei, Phys. Rev. Lett. **28,** 407 (1972).
[7] P. A. Colestock and W. D. Getty, Bull. Am. Phys. Soc. **18,** 1290 (1973).
[8] V. E. Golant, Zh. Tekh. Fiz. **41,** 2492 (1971) [Sov. Phys.—Tech. Phys. **16,** 1980 (1972)].
[9] T. H. Stix, M. Puri, and S. Tutter (private communication).
[10] M. Abramowitz and I. A. Stegun, *Handbook of Mathematical Functions*, Natl. Bur. Stds. Appl. Math. Ser. No. 55 (U. S. Government Printing Office, Washington, D. C., 1964).
[11] I. Fidone, Plasma Physics Laboratory, Princeton University, MATT-979 (1973).
[12] P. A. Colestock (private communication).